Solid State Phenomena Vols. 131-133 (2008) pp. 405-412
online at http://www.scientific.net
© (2008) Trans Tech Publications, Switzerland
Online available since 2007/10/25

Effect of Grown-in Defects on the Structure of Oxygen Precipitates in Cz-Si Crystals with Different Diameter

Litovchenko V.G.[1a], Lisovskyy I.P.[1b], Claeys C.[2c], Kladko V.P.[1d]
Zlobin S.O.[1e], Muravska M.V.[1f], Efremov O.O.[1g], Slobodjan M.V.[1h]

[1]V. Lashkarev Institute of Semiconductor Physics, Nat. Acad. Sci. of Ukraine,
41, Nauky Prosp., Kyiv 03028, Ukraine;
[2]IMEC, Kapeldreef 75, B-3001 Leuven,Belgium
[a]lvg@isp.kiev.ua, [b]lisovsky@isp.kiev.ua, [c]claeys@imec.be, [d]kladko@isp.kiev.ua,
[e]zlobin@isp.kiev.ua, [f]m@isp.kiev.ua, [g]efremov@isp.kiev.ua.

Keywords: silicon, defects, oxygen, precipitates

Abstract. IR-spectroscopy with computer analysis of the shape of the Si-O absorption band, electron microscopy, X-rays diffraction and measurements of unsteady photoconductivity time-decay under band-to band excitation were used to investigate the influence of defects in different diameter (40 – 300 mm) Si ingots on the oxygen precipitation due to two-stage annealing (750 ^{o}C + 1050 ^{o}C). It is shown that large size Cz-Si ingots have a relatively low concentration of electrically active micro-defects, containing small (0.06 – 0.1 μm) dislocation loops. During thermal treatments this leads to the formation of a low stressed oxide phase (SiO_2) with an enhanced thermo-stability. The precipitates in small size ingots, however, contain distorted 4-fold rings of SiO_4 tetrahedra.

Introduction

The oxygen behavior in Cz-Si, important at different processing stages of state-of-the-art technologies, is extensively investigated in the literature [1-4] and is rather good understood. However, in large diameter material produced based on this *know-how* and using optimized crystallization techniques, this matter is studied insufficiently. This is especially the case for nitrogen-doped Si crystals, which are widespread now [3,4]. Further perfection of the Cz-Si production technology is connected with the increased ingot diameter and may influence the material behavior during subsequent thermal treatments. This is the case for the formation of oxygen precipitates, for which structural defect arrangement plays an important role. The latter is of special interest but has not adequately been explored. This work deals with a comparative study of oxygen structural arrangement in Cz-Si ingots with different concentration of grow-in defects.

Experimental technique

The studied (100) oriented and 0.4–0.9 mm thick Cz samples were cut off ingots of various diameter (40–300 mm) and subjected to double-sided polishing. The interstitial oxygen concentration C_o was in the 9-11×10^{17} cm^{-3} range. FZ-Si with 2×10^{15} cm^{-3} oxygen was used as a reference sample.

The absorption band due to stretching Si-O vibrations (transparency minimum near 1100 cm^{-1}) was measured using a computer-assisted differential spectrometer and a Fourier transform infrared spectrometer. The absorption spectra were deconvoluted into Gaussian contributions, using the standard parameters (peak position 1107±1 cm^{-1}, FWHM 33±1 cm^{-1}) of the interstitial oxygen absorption band [2]. The absorption band in the low-frequency spectrum is related to the silicon-oxygen precipitated phase and can be described by a set of Gaussian profiles with characteristic parameters for silicon-oxygen molecular complexes [5-7]. The used parameters are given in

All rights reserved. No part of contents of this paper may be reproduced or transmitted in any form or by any means without the written permission of the publisher: Trans Tech Publications Ltd, Switzerland, www.ttp.net. (ID: 193.17.216.226-19/11/07,08:50:26)

Table 1. Details of the oxygen structural arrangement in the oxide phase determination and a reliability analysis of the mathematical deconvolution results were described previously [7]. The deconvolution accuracy was estimated by the mean square deviation of the sum of Gaussians from the experimental spectrum, and did not exceed 10^{-2}.

Table 1. Parameters of the elementary absorption bands

Band	Maximum position, [cm^{-1}]	FWHM, [cm^{-1}]	Si-O-Si angle	Dominant structural component
O	1107±1	33±1	162°	Interstitial oxygen
P1	1085±1	25±1	142°	6-fold rings of SiO_4 tetrahedra
P2	1060±3	25±2	132°	4-fold rings of SiO_4 tetrahedra
P3	1035±3	25±3	126°	Molecular complex Si-O_2-Si_2

The interstitial oxygen concentration was determined using the intensity of the O elementary band and a conversion factor of 3.03×10^{17} cm^{-3} [2]. The precipitated oxygen concentration was estimated using the intensity of the low-frequency absorption band, determined by the mathematical deconvolution of the spectrum (the sum of the profiles P1-P3) [7].

To obtain the geometrical image of the precipitated phase lattice computer simulations were used. SiO_2 clusters consisting of a mixture of 6-fold and 4-fold (if necessary) rings of SiO_4 tetrahedra contained about 150 atoms. The energy minimization was carried out on the basis of a semi=empirical technique [8]. To determine the type and quantity of grow-in defects the initial samples were Secco etched for 30 min and analyzed using an electron microscope HITACHI S-806.

For the structural characterization also measurement of the diffraction curves (DC) full width at half maximum (FWHM) and the diffuse scattering (DS) of X-rays were used. All the measurements were performed by high-resolution "X'Pert Pro MRD XL Ext" diffractometer using symmetrical 004 reflection of CuKα radiation [9-12]. DS allows to reveal not only microdefects as new phase isolation and precipitates but also point defect clusters, which cannot be observed by electron microscopy. These defects are coherent with the crystal matrix possessing fuzzy boundaries and low gradient of displacement fields. It is known that asymmetrical part of DS shifts the scattering from various microdefects (MD) types in the various part of the reciprocal space around the reciprocal lattice point [11]. Therefore one can not only observe but also classify them.

The lifetime of nonequilibrium carriers (τ) was determined from the time decay of non-stationary photoconductivity under low excitation level. The error did not exceed 10%. The carrier diffusion length L has been calculated using the expression $L=\sqrt{D\tau}$, where the diffusion coefficient D=12 cm^2/s for n- Si and D=36 cm^2/s for p-Si.

To create oxygen precipitates two-step annealing (725 °C – 20 hours and 1050 °C – 5-20 hours) in an Ar ambient was used. After annealing the samples received a 10% HF (10 min.) dip.

Results and discussion

Figure 1 shows examples of absorption spectra deconvolution for initial Cz-Si wafers. For 300 mm ingots the absorption band only contains the Gaussian O profile, as no oxygen precipitates are present. The absorption bands for small diameter (40 and 100 mm) wafers show along with the main O profile also the weak profiles P1 and P2.

Hence, in such ingots some quantity of precipitated oxygen phase is present. The structure of this phase is a mixture of 4-fold and 6-fold rings of SiO_4 tetrahedra. Estimation of the agglomerated oxygen concentration gives a value of about 5×10^{16} cm^{-3}. In other words, during Cz-Si growth by an outdated technology about 5% of oxygen in the ingot was incorporated into micro-inclusions of silicon oxide, resulting in mechanical stresses.

The existence of small etching pits in both types of existence has been revealed by electron microscopy. Their size and concentration are given in Table 2. The pit density in 40 mm samples is significantly (~ 4 times) larger than in the 300 mm samples. The etch pit sizes correspond with those of B-type grown-in microflaws (B-clusters or B-swirls). There are different viewpoints on the nature of such clusters. The most commonly used model postulates that B-clusters consist of small vacancy or interstitial type dislocation loops [13,14]. In Table 2 data for the lifetime and diffusion length of non-equilibrium carriers in initial Si samples are also given. In the case of 40 and 300 mm τ is 6-8 μs and 20-23 μs, respectively. In other words, the lifetime is higher for a lower density of small B-type grown-in defects, in agreement with literature [15,16]. The small grown-in defects observed are effective recombination centers.

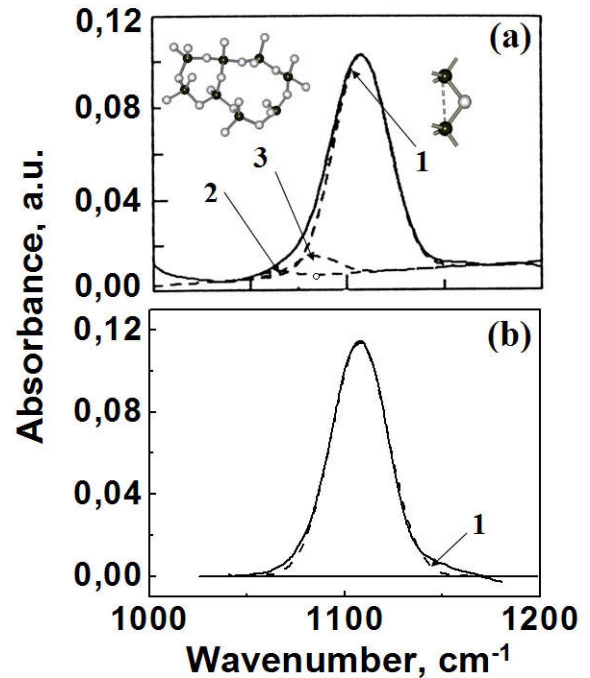

Fig. 1. Si-O absorption band (solid line) and Gaussian contributions (dashed line) for the Cz-Si initial samples with 40 mm (a) and 300 mm (b) diameter. Curves: 1 – interstitial oxygen; 2 – 4-fold rings of SiO_4 tetrahedral; 3 – 6- fold rings of SiO_4 tetrahedral.

Table 2. Defects and electro-physical characteristics of the initial Cz-Si samples

№	Ingot diameter (d), [mm]	Size of etching pits, [μm]	Etch pit density [cm^{-2}]	Lifetime (τ) [μs]	Diffusion length (L), [μm]
1	40	0,05 – 0,1	~2×10^7	6 – 8	85 – 90
2	300	0,05 – 0,1	~5×10^6	20 – 23	265 – 270

In the Table 2 data for the lifetime and diffusion length of non-equilibrium carriers in initial Si samples are also given. In the case of 40 and 300 mm τ is 6-8 μs and 20-23 μs, respectively. In other words, the lifetime is higher for a lower density of small grown-in B-type defects, in agreement with literature data [15, 16]. The small grown-in defects observed are effective recombination centers.

Figure 2 presents the DC from the initial wafers. Their FWHMs are given in Table 3. The samples cut from the large (300 mm) diameter ingot have the minimal FWHM value (δw). As far as the DC FWHM is the integral characteristic of the crystal perfection, these samples are the most perfect. In fact, the value of δw ~ 5 arcsec is very close to the theoretical value. We used the DS analysis to study in detail the origin and parameters of defects. Figure 3(a) and (b) present the DS distribution in the directions perpendicular (q_x-section) and parallel (q_z-section) to the reciprocal lattice vector, where $\boldsymbol{q}$ is the vector from reciprocal lattice node to the point of the measurement. The DS distribution $I(q)$ revealed that all the samples contain both vacancy micro-defects ($q_z < 0$) as well as interstitial ones ($q_z > 0$). Figure 3(b) states that the normalized $I(q)q^3$ value is sensibly constant in the whole q_z range.

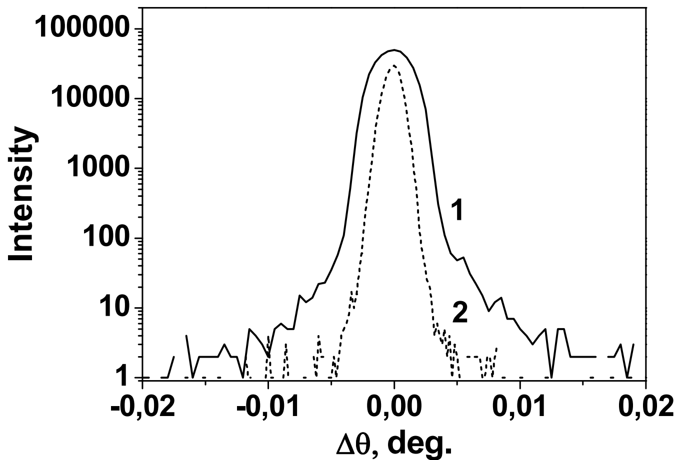

Fig. 2. Diffraction reflection curves for reflex 004 for initial Cz-Si samples cut from ingots of 40 mm (1) and 300 mm (2) in diameter.

This means that the scattering takes place in the asymptotic area, when the defect's power $\boldsymbol{C}$ is proportional to $q >> (QC)^{-1/2}$ [10], where $\boldsymbol{Q}$ – scattering vector. From the point of transition to horizontal part of the scattering dependencies one can easily determine the micro-defects size (see Table 3).The scattering intensity values for the negative q_z are slightly higher than for the positive ones. Therefore the total volume of vacancy defects is larger (about two times) than of the interstitial defects. The intensity behaviour on q_x-section for the 300 mm Si samples shows that the displacement fields are close to the spherical symmetry.

Table 3. Diffraction and structural parameters of the initial Cz-Si samples

N	Ingot diameter (d), [mm]	FWHM, [deg]	MD vacancy type size, [μm]	MD interstitial type size, [μm]
1	40	7.8	0.289	0.278
2	300	5.6	0.220	0.285

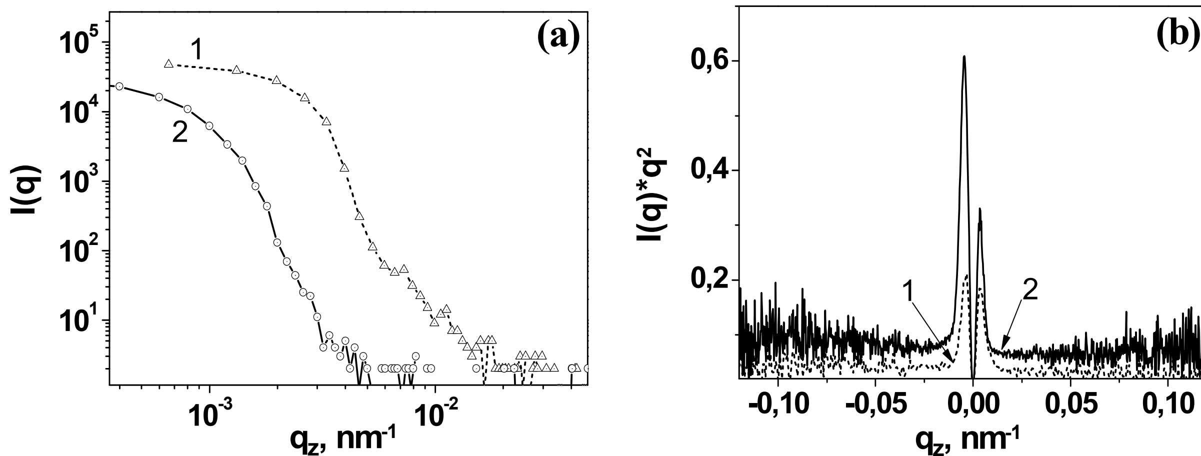

Fig. 3. Intensity of DSXR distribution along q_x-cross-section (a) and q_z-cross-section (b) of the reverse space for centre of 004 for initial Cz-Si samples cut from 40 mm (1) and 300 mm (2) ingots.

The first anneal step (725°C, 20 hours) weakly changed the interstitial oxygen concentration and lead to some increase in oxide phase content (maybe nuclei of the future developed oxygen precipitates). However, the structure of this phase depends on the type of the sample. In the small diameter ingots annealing stimulates primary growth of the oxygen atoms incorporated into 4-fold rings of SiO_4 tetrahedra. Contrary, the large diameter (300 mm) samples are characterized by the appearance of weak-stressed oxide precipitates, which lattice consists of only 6-fold rings of SiO_4 tetrahedra. The concentration of oxygen atoms, which create such a phase, amounts of 4×10^{16} cm^{-3}, i.e., is practically the same as in the initial small diameter ingots. The high temperature (1050°C) treatment essentially decreases the interstitial oxygen concentration in all samples. (Fig. 4). Small diameter ingots are the most effected by the temperature – O_i value decreased for 20 hours of annealing with 75%. In large diameter ingots this effect is weaker (~10%).

Si processing influences essentially the oxygen precipitation process during the high temperature treatment (Fig. 5). For small diameter ingots the concentration of agglomerated oxygen atoms increases and reaches 3.6×10^{17} cm^{-3} after 20 hours of annealing. In the absorption spectrum a new contribution P3 appears along with the P1 and P2 peaks. This contribution is connected with molecular $Si\text{-}O_2\text{-}Si_2$ complexes. It is not excluded that such complexes exist in the Si crystal network independently. However, recent investigation of silicon – thin (10–15 nm) thermal oxide systems by IR spectroscopy and spectral ellipsometry [17], has revealed the existence of such complexes in the interfacial $Si\text{-}SiO_2$ layer. It can be concluded, that in the case of developed oxygen precipitates in Cz-Si the molecular complexes $Si\text{-}O_2\text{-}Si_2$ are most likely localized in the interfacial regions of the silicon – precipitate. In large diameter ingots the high-temperature step of the heat treatment did only marginally lead to changes in content of oxygen precipitates, and in the structure of these precipitates

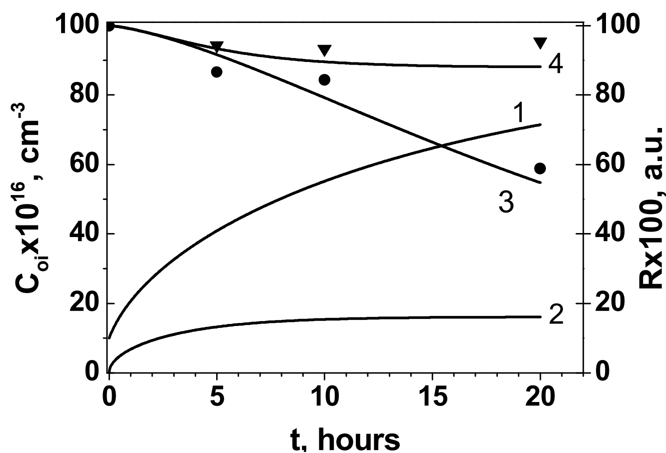

Fig. 4. Dependence of the interstitial oxygen concentration on the anneal time at 1050°C for samples with 300 mm (▼) and 40 mm (●) diameter. Solid lines represent the results of simulation for oxygen release kinetics (curves 3, 4) and for changes in precipitate sizes (curves 1, 2) under high-temperature step of annealing of 40 mm (curves 1, 3) and 300 mm (curves 2, 4) silicon ingots

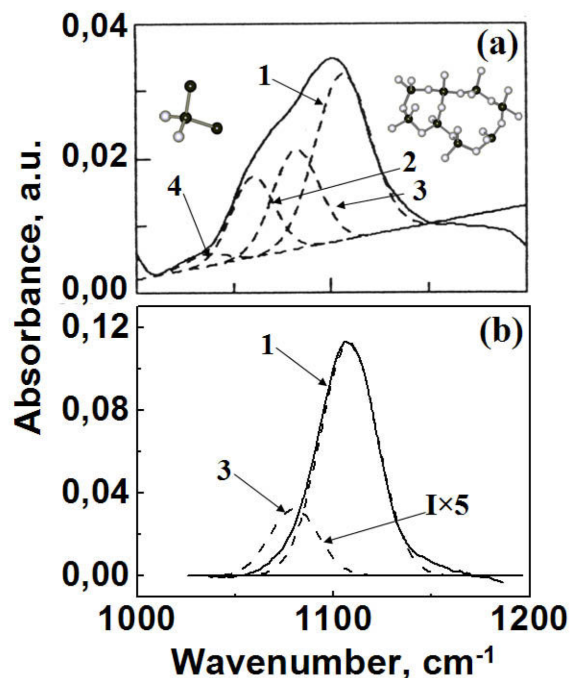

Fig. 5. Si-O absorption band (solid line) and Gaussian contributions (dashed lines) for Cz-Si annealed at 1050°C for 20 h. Figures (a) and (b) correspond to the 40 mm and 300 mm samples, respectively. Curves: 1 – interstitial oxygen; 2 – 4-fold rings of SiO_4 tetrahedral; 3 – 6- fold rings of SiO_4 tetrahedral; 4 –$Si\text{-}O_2\text{-}Si_2$ complex.

Figure 6a shows the results of computer simulations of the SiO_2 structure for the case, when the lattice consists of only 6-fold rings of SiO_4 tetrahedra (large diameter ingots). It is seen that a rather well-ordered structure is formed, which looks like that of low-temperature α-crystobalite [18]. Figure 6b presents the structure of the precipitates in small diameter ingots.

Summering all above mentioned observations one may conclude:

(1) Ingots of small diameter have a large content of small (0.05 – 0.1 μm) grown-in defects, which appear as small dislocation loops of the vacancy type. These defects are electrically active and lead to a degradation of the lifetime and the diffusion length of non-equilibrium carriers.

(2) In such samples under elevated temperatures oxygen precipitation takes place with a high efficiency; it leads to the formation of SiO_2 regions with increased content of stressed 4-fold SiO_4.tetrahedral rings. These regions are surrounded with layers, which contain slightly oxidized silicon (in the form of molecular clusters, for example, $Si\text{-}O_2\text{-}Si_2$).

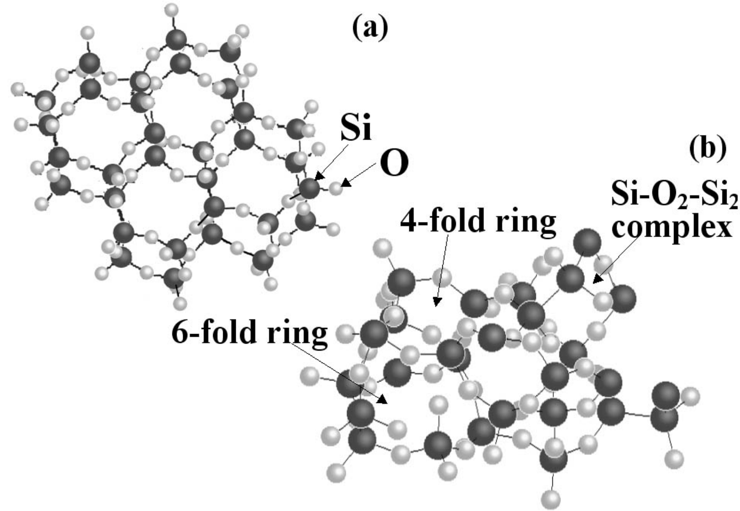

Fig. 6. The image of the structural lattice for oxygen precipitates in large diameter (a) and small diameter (b) ingots.

It is known that the growth and cooling rates of small diameter Si ingots are higher than in the case of large diameter ones. That should lead to the appearance of a large amount of grown-in defects in small diameter ingots and to a decrease of the lifetime and diffusion length of non-equilibrium carriers. These grown-in defects should result in relatively high mechanical stress fields (if compare to large diameter ingots). Naturally, at high temperatures (1050^oC) Si is rather plastic. During cooling-down the mall diameter samples with strain should stimulates the formation of a strongly strained oxide phase, which contains distorted 4-fold rings of SiO_4 tetrahedra.

One may suppose that vacancy defects observed in Si crystals by both electron microscopy and XRD should play the role of oxide phase nuclei during subsequent heat treatments. In this case the following experimental facts become clear: (i) enhanced interstitial oxygen reduction at high temperatures in small diameter samples, because of the great number of sinks for oxygen atoms; (ii) a drastic difference of precipitated phase amount in ingots of small and large diameter.

Let us review in more details the kinetics of the high-temperature anneal step (Fig. 4). One should take into consideration that at the very beginning both kinds of the samples have practically the same content of interstitial oxygen, however, the concentration of the micro-defects in the samples is substantially different. Let us suppose that only existing nuclei of SiO_2 phase connected with structural defects can act as sinks for released oxygen atoms. In that case the simplest equations of mass balance for the release and capture of oxygen at nuclei are:

$$dC_i/dt = -\, dC_p/dt = k_{i\to b}°(C_i - C_{if})°N_p \quad (1)$$

$$dR^2/dt = 2D°(C_i - C_{if})/(C_{pr} - C_{if}) \quad (2)$$

where $k_{i\to b} = 4\pi DR$ – reaction constant for diffusion-limited process of growth/decomposition of a precipitate with radius R; D – diffusion coefficient, C_{pr} – oxygen concentration in SiO_2 phase, C_i – current concentration of interstitial oxygen, N_p – the number of precipitates per volume unit, and C_{if} – equilibrium concentration of the mobile oxygen atoms near the curved SiO_2/Si interface.

Taking into account the Gibbs-Thomson effect, the latter value may be written as:

$$C_{if} = C_{eq}\exp(2\gamma\Omega/Rk_BT) \approx C_{eq}(1+2\gamma\Omega/Rk_BT) \quad (3)$$

where γ – interface specific free energy, Ω – oxygen atomic volume in created precipitate phase, T – annealing temperature, C_{eq} – equilibrium oxygen solubility in silicon at given temperature, k_B – Boltzman’s constant.

Apparently the influence of curvature is remarkable for the first stage of nuclei growth and is rather small for high temperatures (second step of annealing). However it should be desirable to consider the fact, that nucleation and growth of the SiO_2 phase depends on the presence of the point defects (that is a consequence from Vanhellemont – Claeys's formula [19] for the critical radius R_c). For the moment we took only into account the simplest form, supposing that growth ($C_{if} < C_i$) took place if $R>R_c$ (R_c is smaller when the precipitate surrounding is saturated with excess vacancies). Furthermore, we did not take into consideration decomposition of the sub-critical nuclei ($C_{if} > C_i$, $R<R_c$), supposing that this faster process is connected with the earlier step of annealing and can not influence the experimental kinetics curve. Thus, let us suppose that our system consists of the same supercritical nuclei with radius R and concentration N_p, which are surrounded with interstitial oxygen with concentration C_i. The interface concentration C_{if} is considered as a free parameter, which qualitatively reflects the defect arrangement and should be determined.

In Fig. 4 the calculated kinetics of interstitial oxygen concentration decay and of precipitate radius growth is compared with experimental data for the ingots of different diameter. Parameters of calculations are the following: initial nuclei radii ratio R_{40}/R_{300} = 0.1/0.001 (here and further indexes correspond to ingot diameter); precipitates concentrations ratio N_{p300}/N_{p40}=25. Equilibrium oxygen concentrations at the SiO_2/Si interface were estimated from experimental data and the corresponding ratio was C_{if300}/C_{if40} ~9.

Results of calculations enable us to make several principal conclusions:

- large-diameter ingots possess a high amount of very small oxygen precipitates which are well-combined with silicon matrix (the final radii of precipitates for large- and small-diameter ingots range 1:5);
- the amount of fixed oxygen in large-diameter ingots after annealing is about 4x lower than in small-diameter ingots;
- precipitates in large-diameter ingots possess more efficient (up to 5 times) gettering properties.

Conclusions

Oxygen precipitates in small diameter ingots are characterized by the presence of strongly strained SiO_4 tetrahedra rings. Their relieved decomposition as a result of mechanical stresses during thermal relaxation is one of the reasons of thermo- and other types of instabilities. Contrary, large diameter Si ingots contain a relatively low concentration of electrically active grown-in micro-defects, which are small (0.06 – 0.1 μm) dislocation loops, mainly of the vacancy type. These defects lead to a higher thermal stability as a result of the formation of a slightly stressed oxygen phase (SiO_2).

References

[1] K. Tempelhoff, F. Spiegelberg, R. Gleichmann, D. Wruck. Phys. Stat. Sol. (a). Vol. 56 (1979), p.213–223.

[2] B. Pajot, H.J. Stein, B. Cales, C. J. Naud. Electrochem. Soc. Vol.132 (1985), p.3034–3037.

[3] K. Nakai, Y. Inoue, H. Yokota, et al. J. Appl. Phys. Vol. 89 (2001), p.4301–4309.

[4] A.A. Efremov, V.G. Litovchenko, A.V. Saricov, H. Richter, V. Akhmetov. Solid St. Phenom. Vol. 95 –96 (2004), p.405–408.

[5] I.P. Lisovskyy, V.G. Litovchenko, V.B. Lozinskii et al. Thin Solid Films. Vol. 213 (1992), p.164–169.

[6] I.P. Lisovskyy, V.G. Litovchenko, V.B. Lozinskii et al. J. Non-Cryst. Solids. Vol. 187 (1995), p.91–95.

[7] I.P. Lisovskyy. Ukr. J. phys. Vol. 42 (1997), p.1260–1265.

[8] J.G. Vinter, A. Davis, M.R. Saunders. J. J. Comput.-Aided Mol. Des., Vol.1 (1987), p. 31-51.

[9] V.T. Bublikh, K.D. Scherbachev. Crystallography. Vol.42 (1997), p.326-330.

[10] V.A. Khrivoglaz: *Diffraction of X-rays and thermal neutrons in non-ideal crystals* (Naukova Dumka, Kiev 1983).
[11] V.T. Bublikh, K.D. Scherbachev. Crystallography . Vol. 39 (1994), p.1105-1111 (in Russian).
[12] V.P. Kladko, L.I. Datsenko, J. Bak-Misiuk, S.I. Olikhovskii, V.F. Machulin, I.V. Prokopenko, V.B. Molodkin, Z.V. Maksimenko. J. Phys. D: Appl. Phys. Vol. 34 (2001), p.A87–A92.
[13] K. Ravey: *Defects and impurities in semiconductor silicon* (Mir, Moscow 1984).
[14] V.G. Litovchenko. Semiconductor technique and microelectronics. Vol.33 (1981), p. 3-17.
[15] A. Usami, K. Okura, T. J. Maki. Phys. D: Appl. Phys., Vol.10 (1977), p. 63.
[16] I.M. Greskov, B.V. Smirnov, S.P. Solovjov, et al Semiconductors. Vol. 12 (1978), p.1879-1882.
[17] A. Szekeres , A. Paneva, S. Alexandrova , I. Lisovskyy , V.G. Litovchenko, D. Mazunov. Vacuum. Vol. 69 (2003), p. 355–360.
[18] A.G. Revesz. Phys. Stat. Sol. Vol. 57 (1980), p. 235-243.
[19] J. Vanhellemont and C. Claeys. Appl. Phys. Vol. 62 (1987), p. 3960-3971.